Observation of Single Colloidal Platinum Nanocrystal Growth Trajectories

Haimei Zheng, *et al.*

Science **324**, 1309 (2009);
DOI: 10.1126/science.1172104

I picked up this article to stimulate
"crystal growth seminar". However,
to understand the importance of this matter,
we have to learn some background.

Quantum dot

From Wikipedia, the free encyclopedia

A **quantum dot** is a semiconductor whose excitons are confined in all three spatial dimensions. As a result, they have properties that are between those of bulk semiconductors and those of discrete molecules.[1][2][3] They were discovered by Louis E. Brus, who was then at Bell Labs. The term "Quantum Dot" was coined by Mark Reed.

Researchers have studied quantum dots in transistors, solar cells, LEDs[4], and diode lasers. They have also investigated quantum dots as agents for medical imaging and hope to use them as qubits.

Colloidal nanocrystals

- Chemically synthesized Quantum Dots
- Low fabrication costs with high throughput
- Low dimensions – strongly size-dependent optical behavior
- Thermal stability
- Full tunability from UV to IR

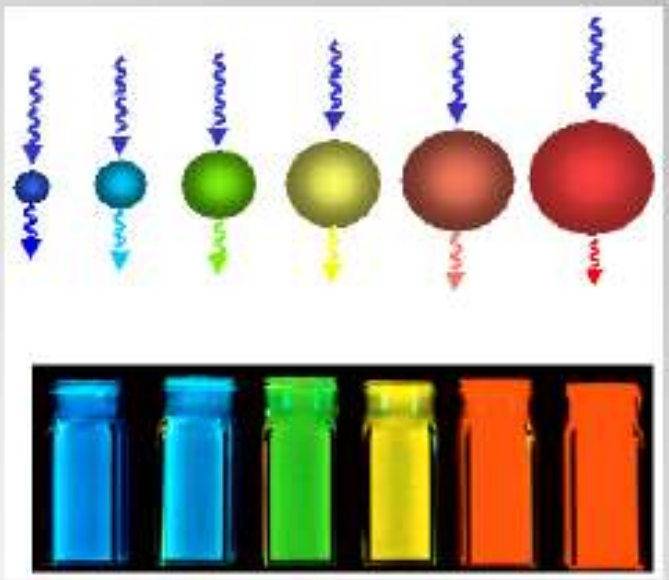

NNL

Scuola Superiore ISUFI

Colloidal nanocrystals

- Chemically synthesized Quantum Dots
- Low fabrication costs with high throughput

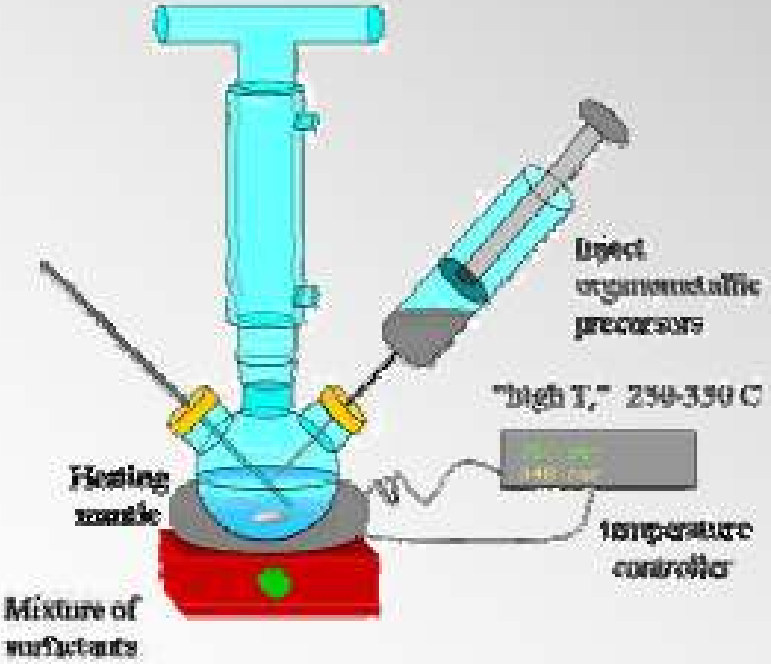

Colloidal nanocrystals

- Chemically synthesized Quantum Dots
- Low fabrication costs with high throughput

MOCVD

MBE

Building blocks for photonic devices

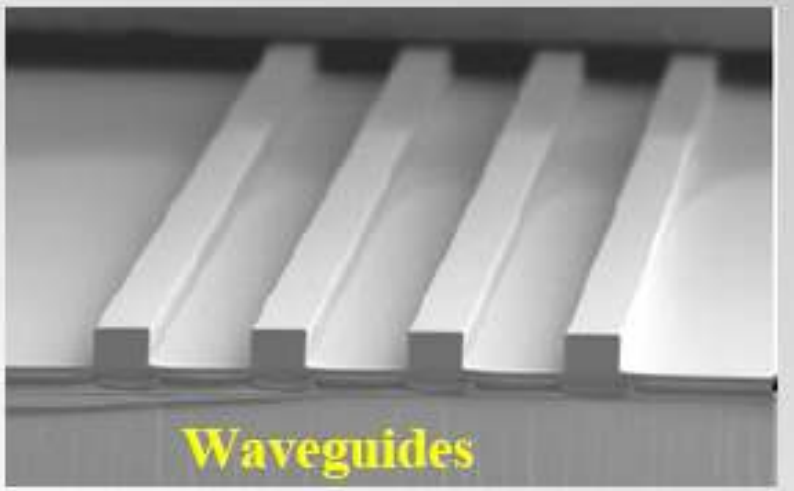

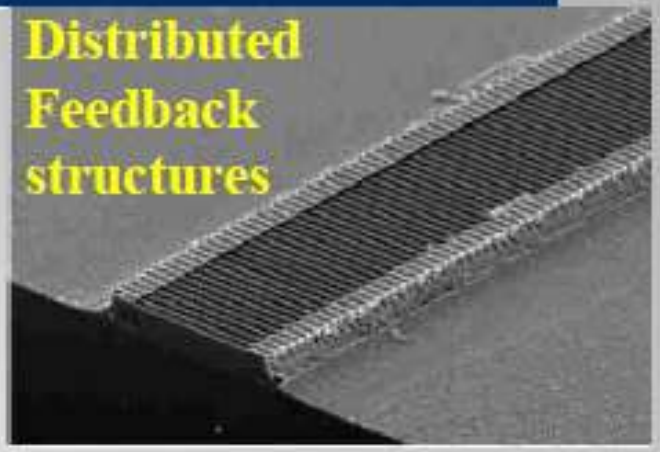

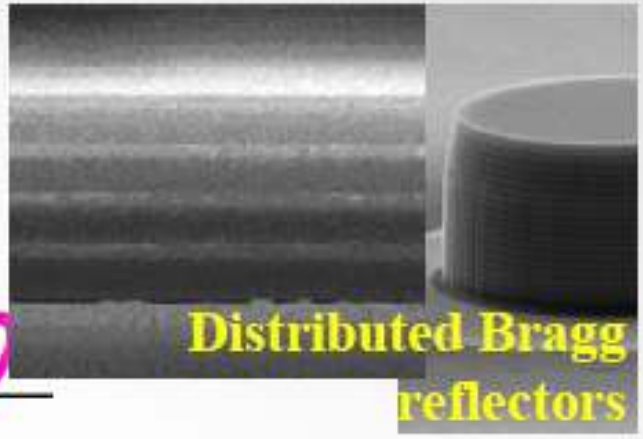

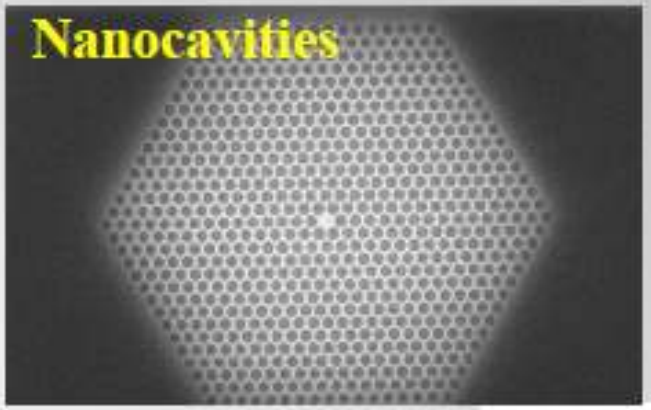

NNL

Scuola Superiore ISUFI

INSIGHT REVIEW NATURE|Vol 437|29 September 2005|doi:10.1038/nature04165

Colloidal nanocrystal synthesis and the organic–inorganic interface

Yadong Yin[1] & A. Paul Alivisatos[1]

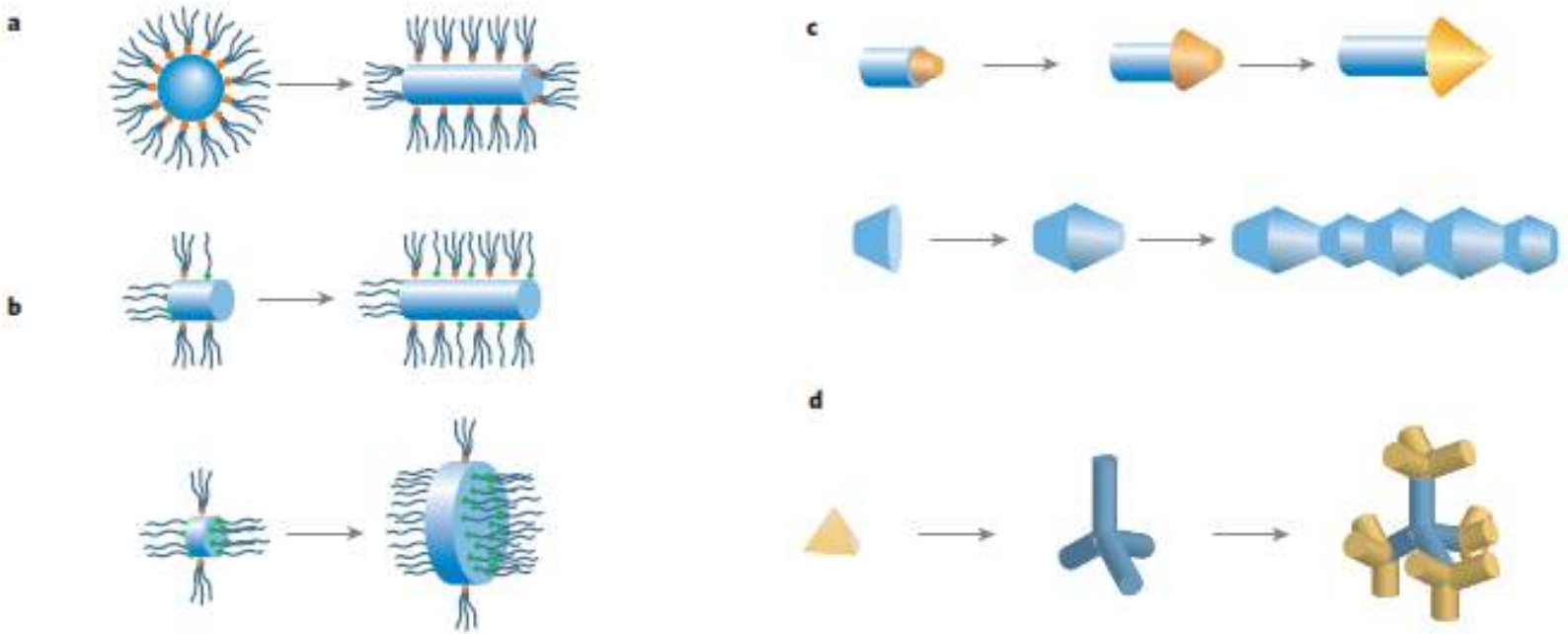

Figure 1 | Shape control of colloidal nanocrystals. **a**, Kinetic shape control at high growth rate. The high-energy facets grow more quickly than low-energy facets in a kinetic regime. **b**, Kinetic shape control through selective adhesion. The introduction of an organic molecule that selectively adheres to a particular crystal facet can be used to slow the growth of that side relative to others, leading to the formation of rod- or disk-shaped nanocrystals. **c**, More intricate shapes result from sequential elimination of a high-energy facet. The persistent growth of an intermediate-energy facet eventually eliminates the initial high-energy facet, forming complex structures such as an arrow- or zigzag-shaped nanocrystals. **d**, Controlled branching of nanocrystals. The existence of two or more crystal structures in different domains of the same crystal, coupled with the manipulation of surface energy at the nanoscale, can be exploited to produce branched inorganic nanostructures such as tetrapods. Inorganic dendrimers can be further prepared by creating subsequent branch points at the defined locations on the existing nanostructures. The red and green dots in **a** and **b** represent metal coordinating groups with different affinities to nanocrystal facets.

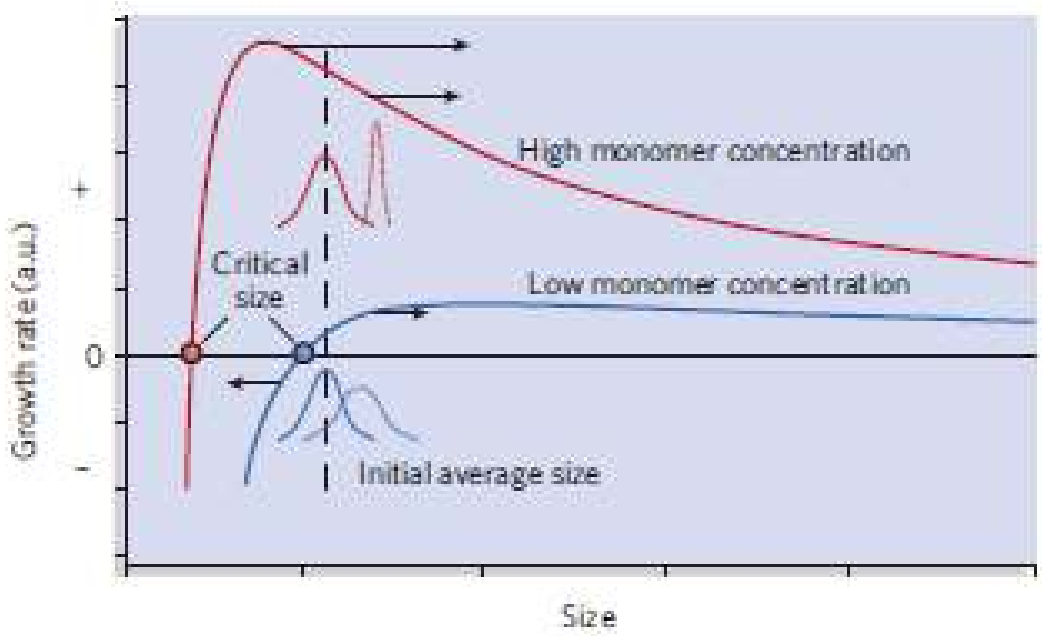

Figure 2 | Size-distribution focusing. The growth process of nanocrystals can occur in two different modes, 'focusing' and 'defocusing', depending upon the concentration of the monomer present. A critical size exists at any given monomer concentration. At a high monomer concentration, the critical size is small so that all the particles grow. In this situation, smaller particles grow faster than the larger ones, and as a result, the size distribution can be focused down to one that is nearly monodisperse. If the monomer concentration is below a critical threshold, small nanocrystals are depleted as larger ones grow and the size distribution broadens, or defocuses. The preparation of nearly monodisperse spherical particles can be achieved by arresting the reaction while it is still in the focusing regime, with a large concentration of monomer still present. a.u., arbitrary units.

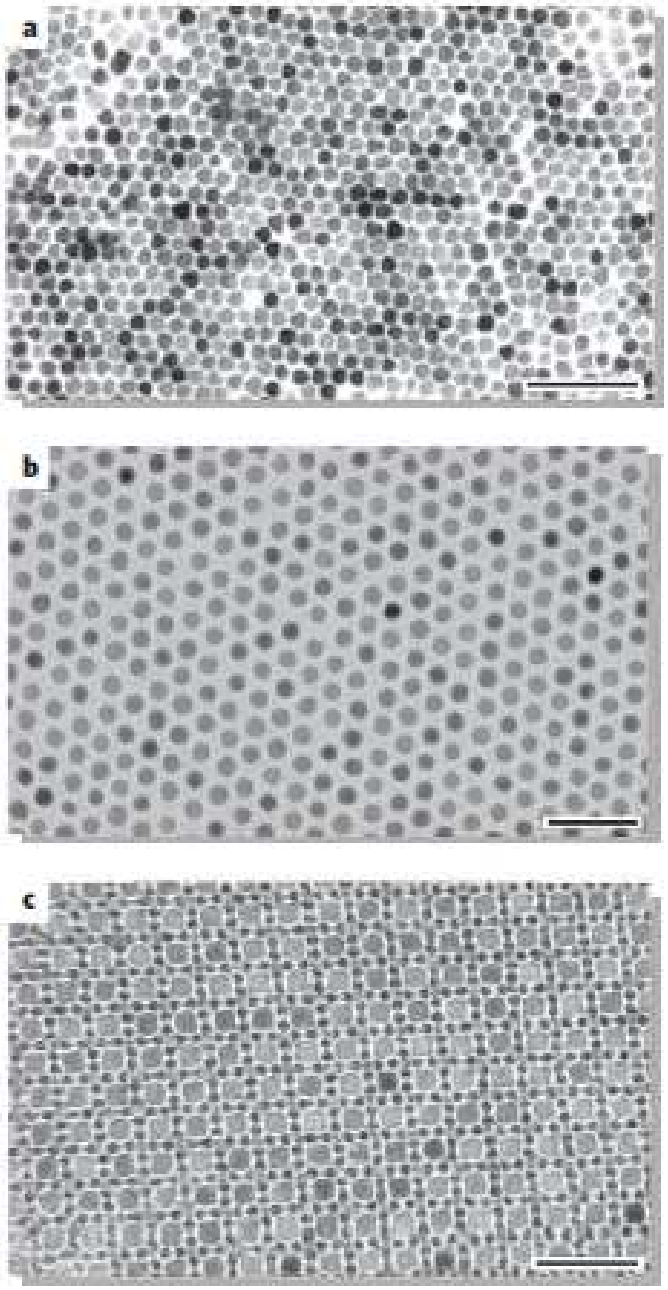

Figure 3 | Monodisperse colloidal nanocrystals synthesized under kinetic size control. **a**, Transmission electron microscopy (TEM) image of CdSe nanocrystals. **b**, TEM image of cobalt nanocrystals. **c**, TEM micrograph of an AB_{13} superlattice of γ-Fe_2O_3 and PbSe nanocrystals. The precise control on the size distributions of both nanocrystals allows their self-assembly into ordered three-dimensional superlattices. Scale bars, 50 nm. Reprinted from ref. 27.

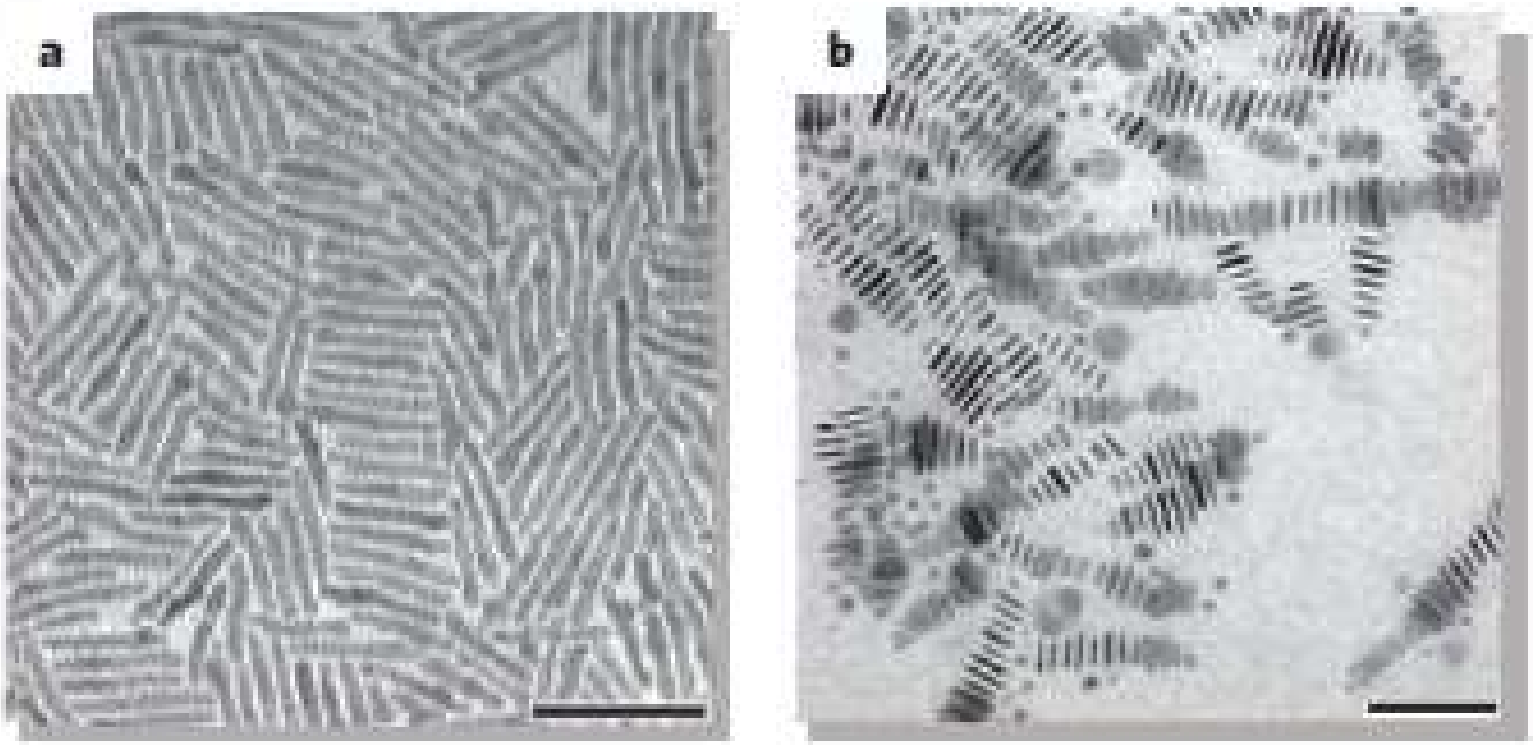

Figure 4 | Anisotropic growth of nanocrystals by kinetic shape control and selective adhesion. **a**, CdSe nanorods (scale bar, 50 nm). Reprinted with permission from ref. 52. **b**, Cobalt nanodisks (scale bar, 100 nm). The organic surfactant molecules selectively adhere to one facet of the nanocrystal, allowing the crystal to grow anisotropically to form a rod or disk.

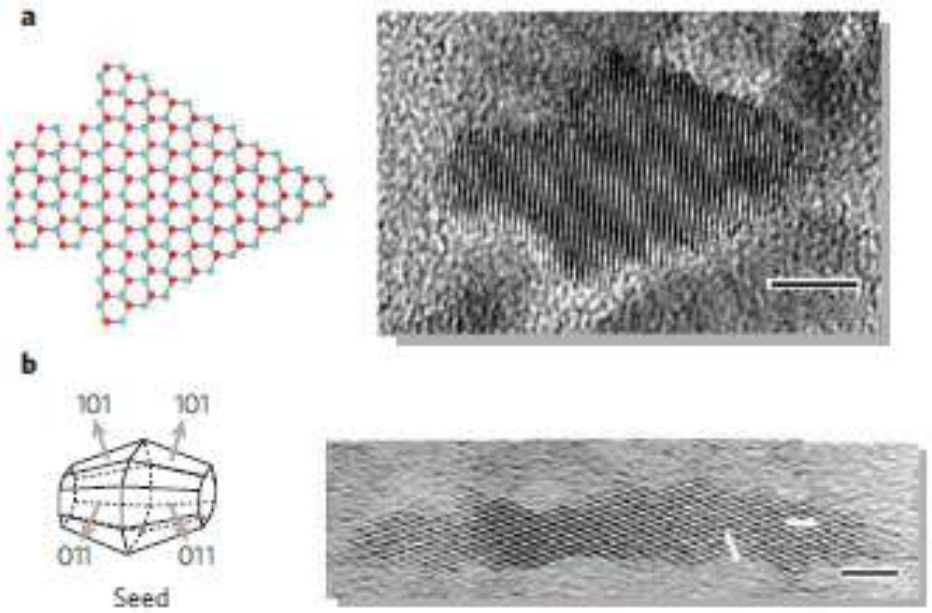

Figure 5 | Nanocrystals with complex shapes prepared by sequential elimination of a high-energy facet. **a**, Two-dimensional representation and a high-resolution TEM image of an arrow-shaped nanocrystal of CdSe. High-resolution TEM characterization shows that each shape of nanocrystal is predominantly wurtzite and that the angled facets of the arrows are the (101) faces. Scale bar, 5 nm. Red and blue dots represent selenium and cadmium atoms, respectively. Reprinted with permission from ref. 22. **b**, Simulated three-dimensional shape and high-resolution TEM analysis of a TiO_2 rod. The long axes of the nanocrystals are parallel to the *c*-axis of the anatase structure, while the nanocrystals are faceted with (101) faces along the short axes. Hexagon shapes (the [010] projection of a truncated octagonal bipyramid) truncated with two (001) and four (101) faces are observed either at the one end or at the centre of the nanocrystals. Scale bar, 3 nm. Reprinted with permission from ref. 35. Copyright (2003) American Chemical Society.

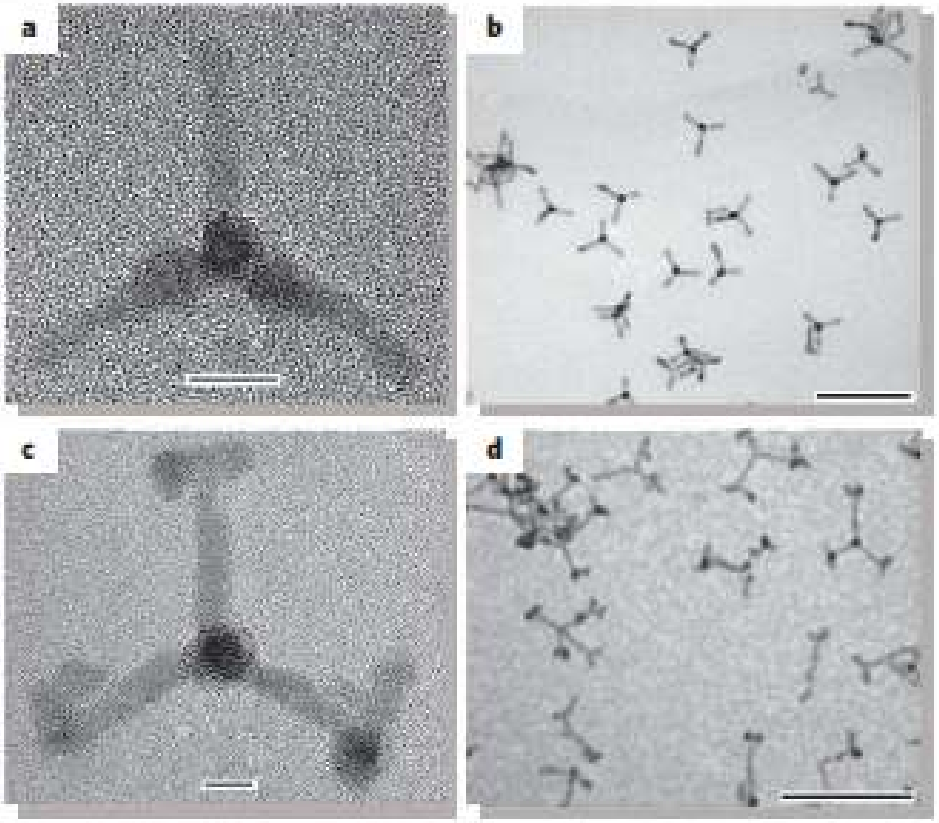

Figure 6 | Controlled branching of colloidal nanocrystals. **a**, High-resolution TEM image of a typical tetrapod-shaped CdSe nanocrystal, looking down the [001] direction of one arm. The nucleus is the zincblende structure, with wurtzite arms growing out of each of the four (111) equivalent faces. Reprinted with permission from ref. 22. **b**, Low-magnification TEM image of CdTe tetrapods. Scale bar, 100 nm. Reprinted from ref. 48. **c**, High-resolution TEM image of a tetrapod that has branches growing out of each arm. There are zincblende layers near the ends of the original arms, and the branches are wurtzite with some stacking faults. Reprinted with permission from ref. 22. **d**, TEM image of branched tetrapods result from nucleation of CdTe zincblende branch points on the end of each arm. Scale bar, 100 nm. Reprinted from ref. 51.

THE JOURNAL OF CHEMICAL PHYSICS VOLUME 19, NUMBER 4 APRIL, 1951

The Growth of Uniform Colloidal Dispersions*

HOWARD REISS
Department of Chemistry, Boston University, Boston, Massachusetts
(Received November 6, 1950)

Recently, much interest has been focused upon the preparation of monodispersed colloids using the "growth by diffusion" process. Although these colloids are useful tools in experimental procedures, no well-established reason has been given to explain why the "growth by diffusion "method should produce such uniform dispersions. In this paper it is shown that an assembly of competing particles, growing by diffusion, develop the squares of their radii at equal rates. This condition provides a mechanism leading towards uniformity.

A method, based on this equal square rule, is suggested for the determination of size distributions in polydispersed systems.

Uses for Monodispersed Colloids

*(1) Experimental verification of light scattering theories.[2]
*(2) Standards in light scattering work.[11,12]
*(3) Experimental verification of coagulation theories.[15]
*(4) Measurement of Avogadro's number.[16]
*(5) Experimental study of the relation between particle size and particle retention in the human lung.[7]
*(6) Measurement of diffusion coefficients in supersaturated solutions.[8,9]
(7) Experimental verification of theories on surface thermodynamics.[14]
(8) Meteorological applications. (In progress.) Unpublished work by V. K. La Mer.
*(9) Studies of reaction kinetics.[13]

Observation of Single Colloidal Platinum Nanocrystal Growth Trajectories

Haimei Zheng, *et al.*

Science **324**, 1309 (2009);
DOI: 10.1126/science.1172104

I picked up this article to stimulate
"crystal growth seminar". However,
to understand the importance of this matter,
we have to learn some background.

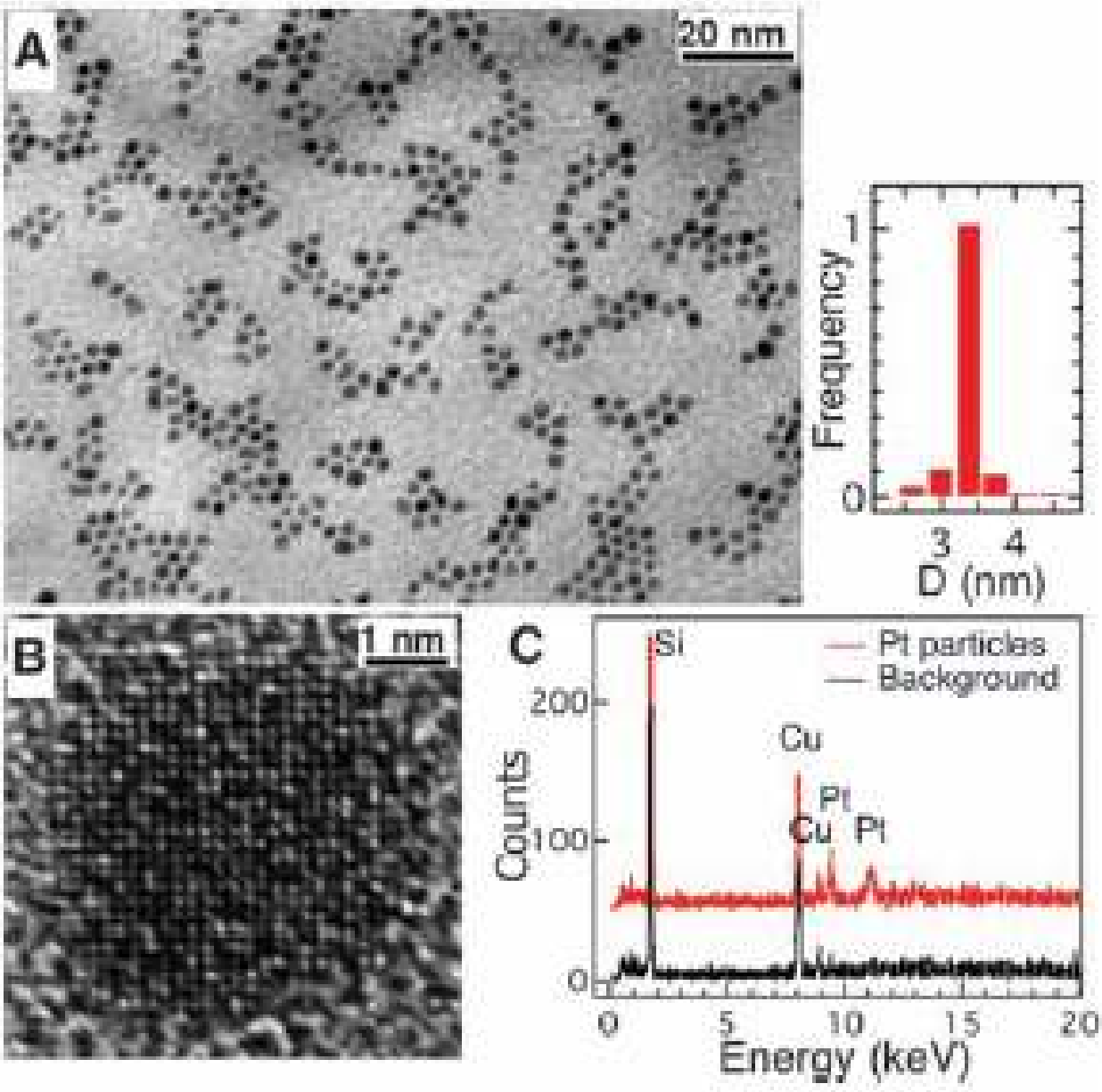

Fig. 1. TEM of Pt nanocrystals synthesized in a liquid cell. (**A**) Bright-field TEM image of Pt nanocrystals with a histogram of particle size distribution, obtained from measurements of 150 particles. (**B**) High-resolution TEM image of a Pt nanocrystal, which was recorded after the in situ experiment. (**C**) EDS spectra from Pt nanocrystals (red) and background (black) obtained ex situ from the same liquid cell. The observed Si and Cu signals are from the silicon nitride membrane window and the cover of the liquid cell, respectively.

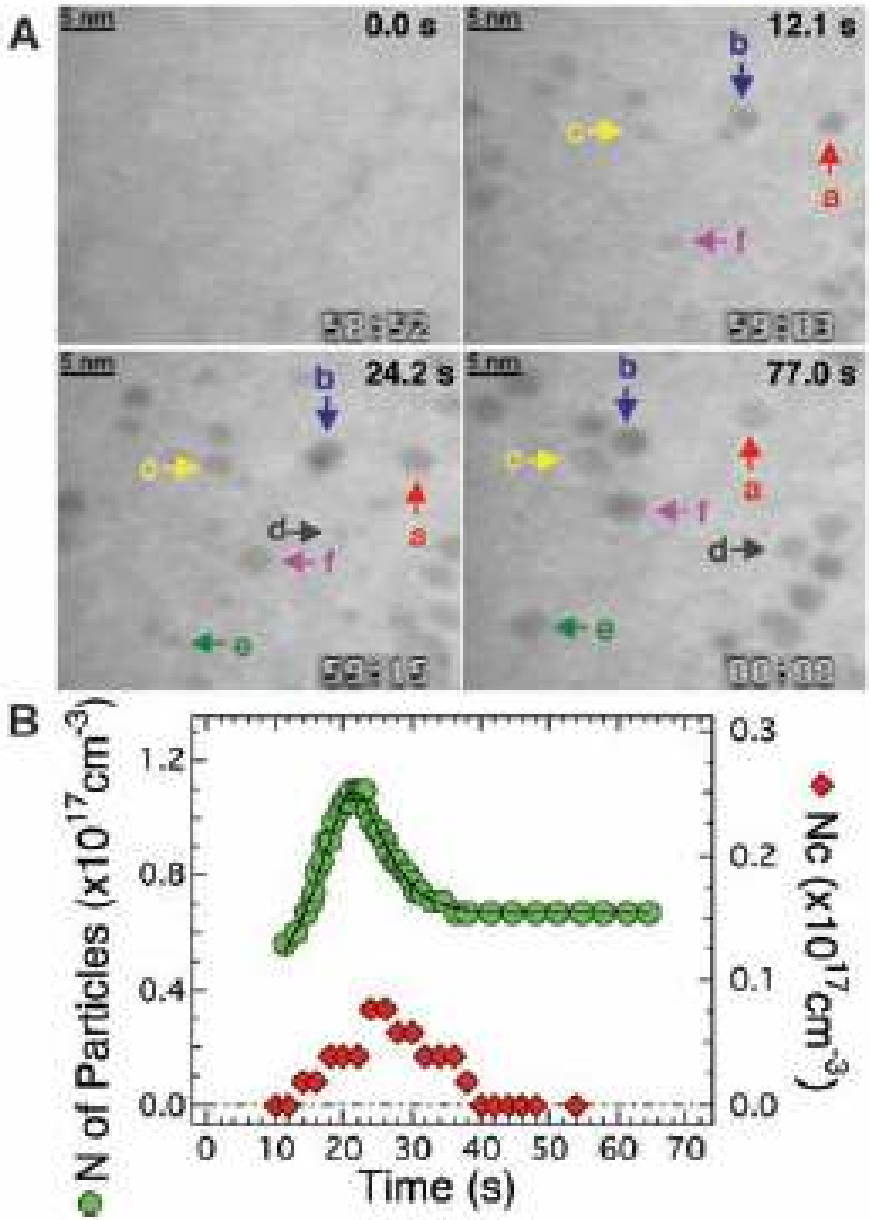

Fig. 2. Growth and coalescence of Pt nanocrystals. (**A**) Video images acquired at 0.0 s, 12.1 s, 24.2 s, and 77.0 s of exposure to the electron beam. Specific particles are labeled with arrows. The growth trajectories of these individual particles reveal the multiple pathways leading to size focusing. (**B**) Number of particles (left axis) and number of coalescence events (Nc, right axis) during an interval of 2.0 s versus time. Particles nucleate and grow during the adjustment of focus for imaging (0 to 10 s), the details of which were not available.

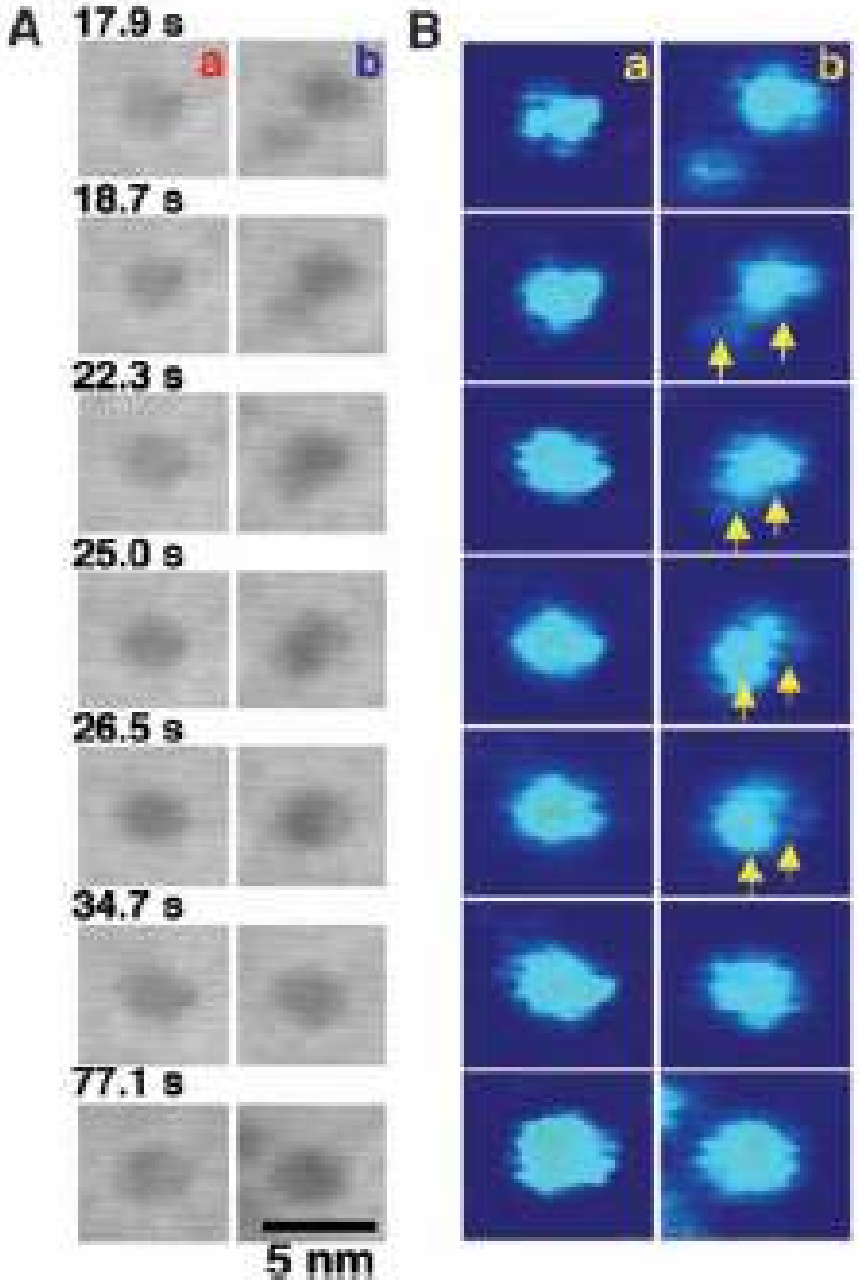

Fig. 3. Comparison of different growth trajectories. (**A**) Video images showing simple growth by means of monomer addition (left column) or growth by means of coalescence (right column). Particles are selected from the same field of view. (**B**) Enlarged (1.5 times) color images of (A). Distinct contrast changes are highlighted with arrows indicating recrystallization, which were observed in the coalesced particle but not in the case of simple growth.

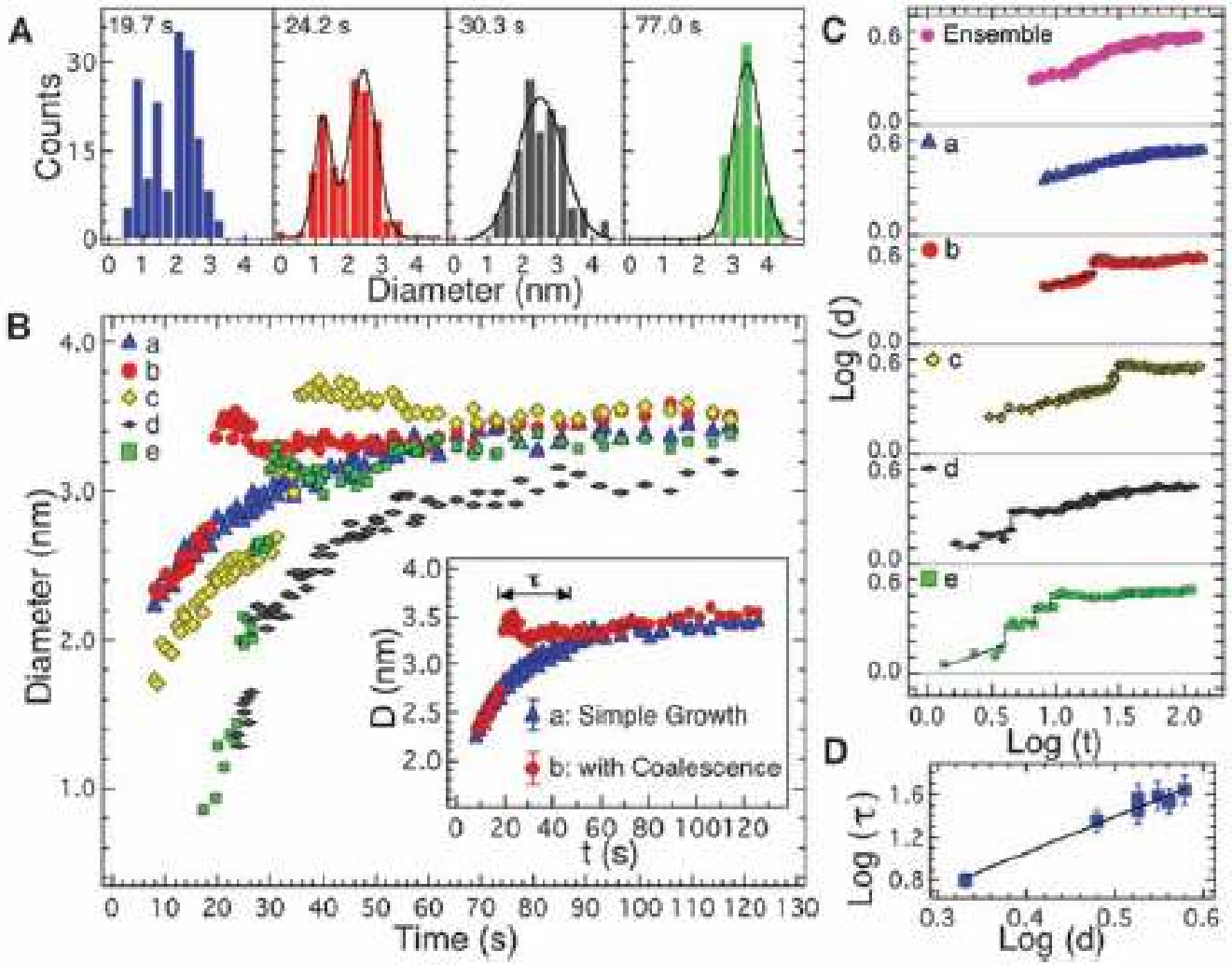

Fig. 4. Growth kinetics of Pt nanoparticles. (**A**) Histograms of particle size distribution at 19.7 s, 24.2 s, 30.3 s, and 77.0 s. Black curves are Gaussian fits. (**B**) Particle size versus growth time. These particles are highlighted in Fig. 2A. Inset shows two types of growth trajectories. A relaxation time (τ) was observed after a coalescence event. Error bars for particle diameter measurements are less than ±0.18 nm. (**C**) Logarithmic relationship of particle size versus growth time for the ensemble and those individual particles in (B). Black lines are guides for the eye, and dashed lines show the coalescence events. (**D**) Logarithmic relationship of relaxation time versus the size of the coalesced particles. Black line shows linear fit.

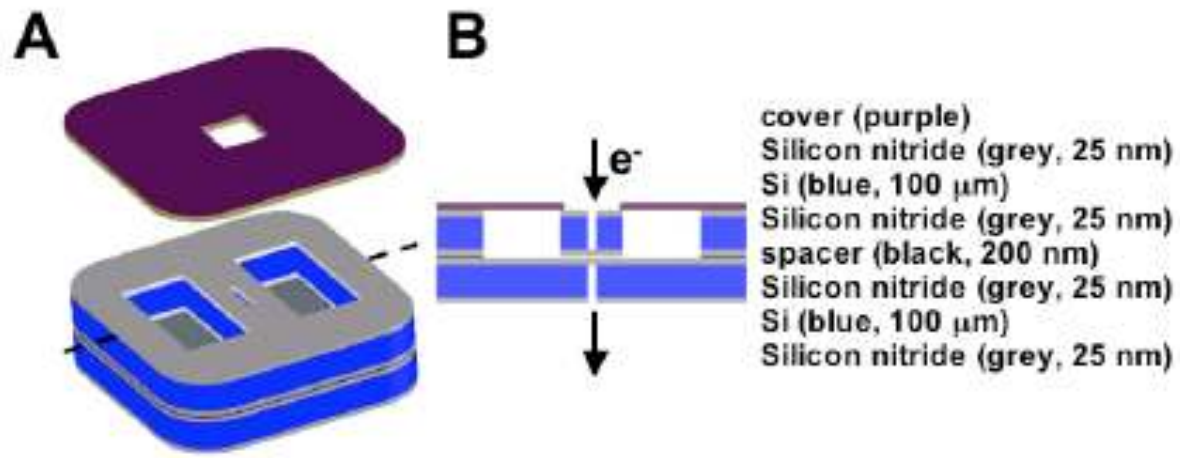

Fig. S1. A liquid cell schematic. (A) Three-dimensional view. Lateral dimensions of the liquid cell: 2.6×2.6 mm and 3 mm in diagonal; reservoirs: 0.6×1.2×0.1 mm; the electron transparent window: 1×50 μm; cover: 0.6×0.6 mm for the hole and its outer dimensions are the same as the liquid cell. (B) Cross-sectional view of the plane marked in (A).

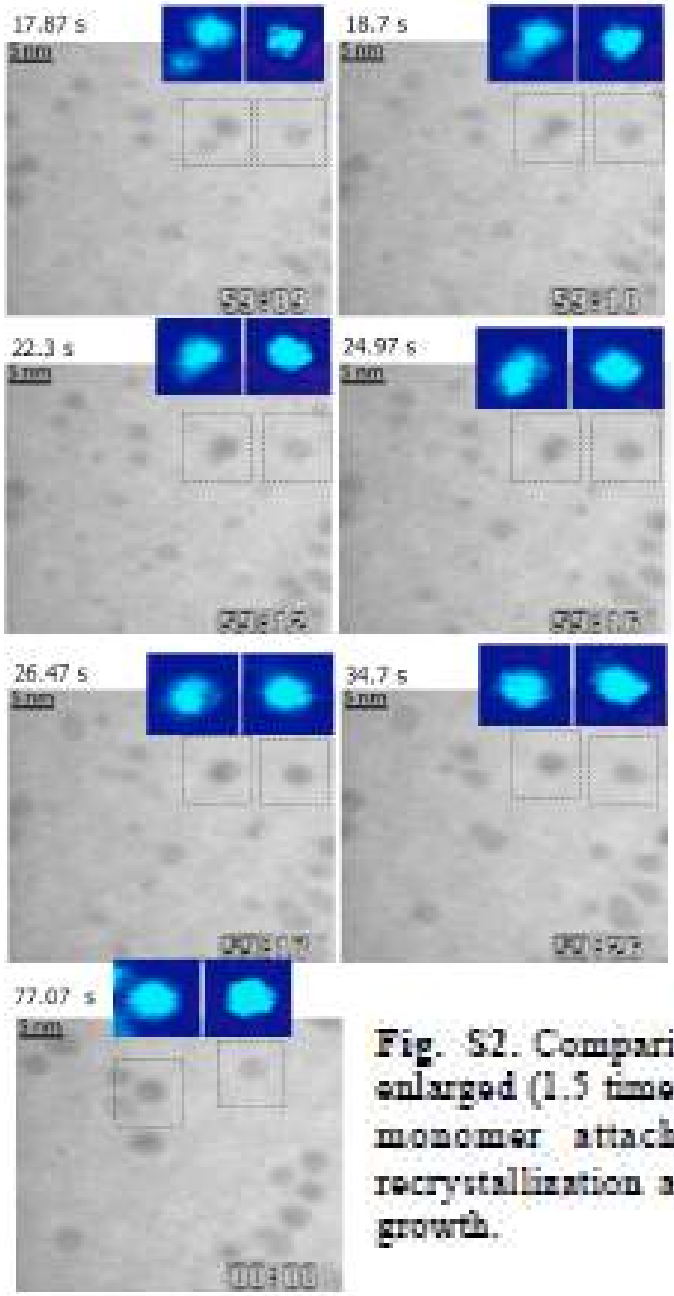

Fig. S2. Comparison of different growth trajectories. The selected particles with the enlarged (1.5 times) color images show two types of growth, either by simple growth of monomer attachment or coalescence. Distinct contrast changes indicating recrystallization are observed in the coalesced particle but not in the case of simple growth.

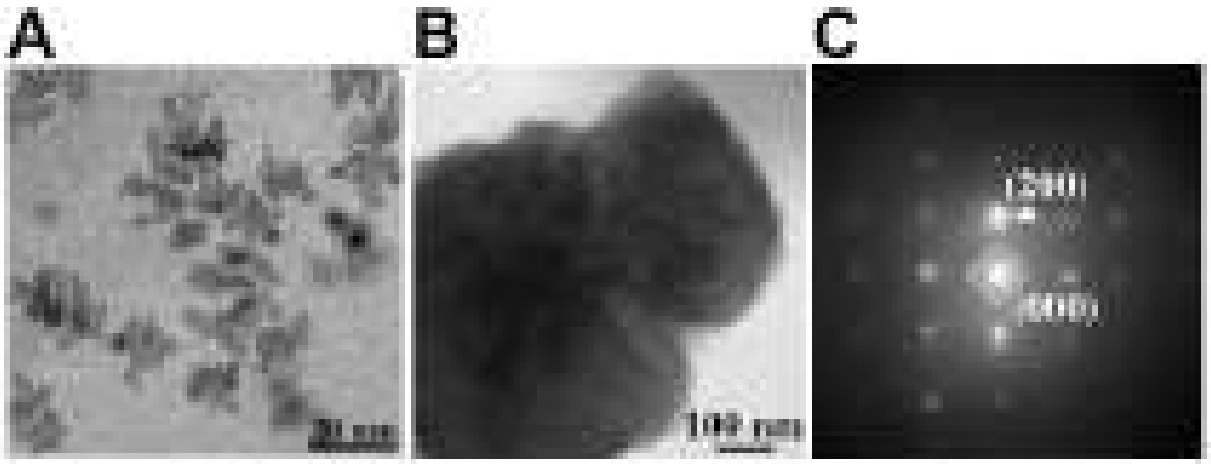

Fig. 53. Formation of platinum dendrites and "foil" when the volume fraction of oleylamine was decreased (0-3%) in the growth solution. A. Platinum dendrites. B. Platinum "foil" was observed in some cases when no oleylamine surfactant was used. C. Selected area diffraction from (B) showing platinum "foil" is crystalline with a face centered cubic structure.